CHEMICAL ENGINEERING TRANSACTIONS
VOL. 103, 2023
A publication of AIDIC
The Italian Association of Chemical Engineering
Online at www.cetjournal.it
Guest Editors: Petar S. Varbanov, Panos Seferlis, Yee Van Fan, Athanasios Papadopoulos

ISBN 979-12-81206-02-1; **ISSN** 2283-9216
DOI: 10.3303/CET23103023

Investigation of Fluid Flow and Heat Transfer Around Smooth Sphere with the LES Method

Haonan Jia, Yuhang Tian, Xing Tian, Jian Yang*, Qiuwang Wang

MOE Key Laboratory of Thermo-Fluid Science and Engineering, Xi'an Jiaotong University, Xi'an 710049, China
yangjian81@mail.xjtu.edu.cn

Fluid flow around the sphere is widely used in industrial systems, in which the hydrodynamic and heat transfer performances play a key role in energy consumption. The flow and heat transfer characteristics around the sphere are greatly dependent on the shedding and development of vortices. In the present paper, the fluid flow and heat transfer around the smooth sphere are investigated with the LES method. The results show that along the flow direction, the leeward region of the sphere alternately produces up and down-shedding vortices. Vortex shedding causes local pressure changes, resulting in changes in flow and heat transfer performance. The C_d, C_L, and *Nu* fluctuate around a stable value. The frequency and amplitude of the fluctuation increase significantly as the inlet flow rate increases. Especially, the maximum changes in C_d are 6.26 % and 22.79 % when Q = 1 and 6 m^3/h. The frequency of vortex shedding increases by about 2.6 times when the flow rate increases from 2 m^3/h to 5 m^3/h. In addition, the vortex shedding from the leeward region moves downstream with more energy due to the increase in frequency, which leads to more cold fluid participating in heat transfer.

1. Introduction

Flow past the bluff body appears widely in wind engineering, coastal engineering, chemical engineering, ground transportation, aerospace, and other fields. Therefore, flow around the bluff body and unsteady wakes are some of the traditional research topics in fluid mechanics. The blunt body can be divided into a cylinder and a sphere, in which the flow around the sphere exists in many fields. Nessia et al. (2022) experimentally demonstrated a rotating packed bed for nanoparticle production. Tian et al. (2022) investigated the moving packed bed with spherical particles, which is the key equipment in waste energy recovery and concentrated solar power. Wu et al. (2020) investigated the application of spherical particle-packed beds in methane steam reforming for hydrogen production. Therefore, flow around the sphere is a classic research problem in the industry.

Although there were more scholars who researched the flow around the sphere, the critical value of wake vortices for flow around the sphere with different Reynolds numbers was not a uniform conclusion by comparing with the flow around the cylinder. As a typical research, Sakamoto and Haniu (1990) experimentally investigated the vortex shedding from spheres at Reynolds numbers from 3×10^2 to 4×10^4 in a uniform flow. Results showed that the higher and lower frequency modes of the Strouhal number coexist at Reynolds numbers ranging from 8×10^2 to 1.5×10^4. However, Cocetta et al. (2021) obtained that the flow reaches a steady state when Re = 200, and the flow leads to periodic hairpin vortex shedding when Re = 300 by numerical simulation. It was shown that the critical values of the vortex-shedding state were different for the flow around the sphere.

On the basis of investigating the flow characteristics of flow around the sphere, scholars gradually pay attention to the heat transfer performance. Li et al. (2017) found that the spacing-to-sphere diameter ratio had an impact on the flow resistance and Nusselt number for flow around side-by-side spheres by the LES method. The flow and heat transfer characteristics of a particle stacking bed composed of several spherical particles have also been studied. Li et al. (2018) introduced a dimpled structure on the spherical particle surface of the particle-packed bed and compared the flow and heat transfer characteristics of smooth and dimpled particle-packed beds with two different pipe size ratios (N = 1 and N = 1.15) by numerical calculation. The results showed that when the channel-to-particle diameter ratio (N) was 1, the existence of a dimpled structure could reduce the pressure drop by about 5 %, but the *Nu* number was almost unchanged. The pressure drop of the dimpled

Paper Received: 12 April 2023; Revised: 12 July 2023; Accepted: 26 July 2023
Please cite this article as: Jia H., Tian Y., Tian X., Yang J., Wang Q., 2023, Investigation of Fluid Flow and Heat Transfer Around Smooth Sphere with the LES Method, Chemical Engineering Transactions, 103, 133-138 DOI:10.3303/CET23103023

particle-packed bed increased by about 25 %, and the *Nu* increased by about 10 % when *N* = 1.15. When *N* = 1, Yang et al. (2018) found that the increase in dimple depth would reduce both pressure drop and heat transfer. In addition, compared with a smooth particle-packed bed, the existence of a dimpled structure could reduce pressure drop by 10 % - 20 % and heat transfer by 5 % - 15 %. In our previous study (Jia et al., 2021), it was found that when *N* = 1, 1.15, 1.3, and 1.47, the existence of a dimpled structure increased the flow resistance and led to the increase of *Nu* number at the same time. These studies showed that there was no uniform conclusion in the study of packed beds. Therefore, it is necessary to investigate the local flow and heat transfer characteristics of flow around the sphere so as to guide the research of the spheroidal particle-packed bed. Besides, the analysis of the development of the wake region around the sphere can guide the design of the surface structure of the sphere, which has potential in the field of improving heat transfer performance. The flow and heat transfer characteristics of flow around the sphere are investigated by large eddy simulation. The flow resistance coefficient, lift coefficient, Nusselt number, and wake vortex are compared and analysed in detail.

2. Physical model and computation methods

2.1 Physical model

The geometry model used in the simulation is shown in Figure 1. The diameter (*D*) of the sphere is 21 mm, while the size of the channel is 12 *D* (length) × 4 *D* (width) × 4 *D* (height). The 4 *D* length is arranged in front of the sphere in order to make the inlet fluid flow uniformly. The length of 8 *D* can ensure the full development of the wake. The freestream velocity u_0 with 0.5 % turbulence intensity and the constant temperature of T_0=298 K are applied to the domain inlet. The pressure outlet condition with zero-gauge pressure is used at the domain outlet. During the simulation process, the sphere surface is no-slip, with constant temperature boundaries at T_s = 318 K. The square channel walls are no-slip and adiabatic boundaries.

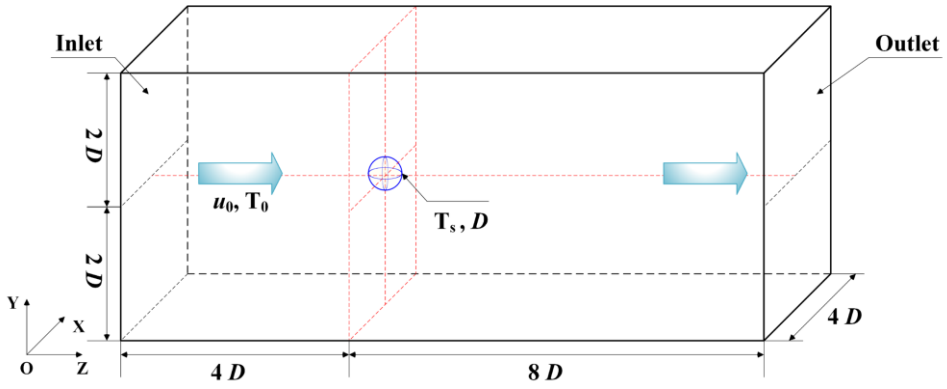

Figure 1: Schematic of flow around the sphere

2.2 Governing Equations and Computational Methods

By performing top hat filtering on the governing equation of the flow field, the incompressible filtering equation of the LES method for solving the field is obtained as follows:

$$\frac{\partial \rho}{\partial t}+\frac{\partial}{\partial x_i}(\rho \overline{u_i})=0 \tag{1}$$

$$\frac{\partial}{\partial t}(\rho \overline{u_i})+\frac{\partial}{\partial x_j}(\rho \overline{u_i}\overline{u_j})=\frac{\partial}{\partial x_j}(\sigma_{ij})-\frac{\partial \overline{p}}{\partial x_i}-\frac{\partial \tau_{ij}}{\partial x_j} \tag{2}$$

$$\frac{\partial \overline{T}}{\partial t}+\frac{\partial}{\partial x_j}\left(\overline{T}\overline{u_j}\right)=\frac{\partial}{\partial x_j}\left(\left(\alpha+\alpha_{SGS}\right)\frac{\partial \overline{T}}{\partial x_j}\right) \tag{3}$$

where $\overline{u_i}$, $\overline{p}$, and $\overline{T}$ are the filtered velocity, pressure and temperature. The τ_{ij} is unknown and must be modelled. In the simulation, the sub-grid scale turbulent stress is calculated based on the Boussinesq hypothesis as follows:

$$\tau_{ij}-\frac{1}{3}\tau_{kk}\delta_{ij}=-2\mu_{t\text{-}sub}\overline{S_{ij}} \tag{4}$$

where the $\mu_{t\text{-}sub}$ is the sub-grid scale turbulent viscosity. In the present simulation, the $\mu_{t\text{-}sub}$ is modelled based on the Smagorinsky-Lilly model.

$$\mu_t=\rho L_s^2\sqrt{2\overline{S}_{ij}\overline{S}_{ij}} \tag{5}$$

where L_s is the mixing length of the sublattice scale.

In the present simulation, all governing equations are solved by using finite volume analysis software Fluent 14.5. The PISO algorithm is employed to couple the velocities and pressure. The boundary central difference scheme is used for the momentum equation, and the second-order implicit scheme is used for the time term. The dimensionless time step is $\triangle tu_0/D$ = 0.02 for the following calculation after the time step independence verification. First, 750-dimensionless time steps are calculated to obtain relatively stable results, and then 3,000-dimensionless time steps are calculated to obtain the data of time-averaged flow and heat transfer characteristics for investigation. In the iterative calculation process, the final residual calculated at each step is less than 10^{-3}.

The Reynolds number (*Re*) in this study is based on the interstitial velocity (u_0) and sphere diameter (D) in the present study. The inlet flow range (Q) studied in this paper is 1 - 6 m^3/h. The range of *Re* is 1,000 – 5,000, which is in the turbulent region. The S is the cross-sectional area of the channel perpendicular to the flow direction.

$$Q=Su_0 \tag{6}$$

$$Re=\frac{\rho u_0 D}{\mu} \tag{7}$$

In order to analyse the flow and heat transfer characteristic of flow around the sphere, the flow resistance (C_d), lift coefficient (C_L), and Nusselt number (*Nu*) are defined as follows:

$$C_d=\frac{F_d}{\frac{1}{2}\rho u_0^2 D} \tag{8}$$

$$C_L=\frac{F_L}{\frac{1}{2}\rho u_0^2 D} \tag{9}$$

$$Nu=\frac{Q}{\pi D(T_s-T_0)\lambda} \tag{10}$$

3. Computational grid and model validations

In this section, taking the flow resistance coefficient as the evaluation parameter, the grid independence of the main stream and the sphere surface are verified. There is a small difference in the calculation results when the mesh size of the mainstream area is 1/12 D and the sphere surface is 1/24 D. The grid details near the sphere surface is shown in Figure 2. The results are compared with the simulation and experimental studies of Dixon et al. (2011), Ranz and Marshall (1952) and Whitaker (1972). The average errors of C_d and *Nu* are 2.70 % and 4.17 %, and the maximum errors are 3.17 % and 7.20 %.

Figure 2: Grid details near the sphere surface

4. Results and discussion

In this section, the flow and heat transfer characteristics of flow around the sphere are analysed. The C_d of flow around sphere at Q = 1, 2, 3, 4, 5, and 6 m^3/h are shown in Figure 3. The flow resistance is mainly due to the pressure difference when flowing around the sphere. The change of C_d over time indicates that the pressure difference at the upstream and downstream regions is unstable. The vortex shedding is an unstable state after the flow around the sphere. The time-averaged C_d are 0.783, 0.679, 0.617, 0.603, 0.576, and 0.576 when Q = 1, 2, 3, 4, 5, and 6 m^3/h. The C_d fluctuation frequency and the maximum deviation increase with the increase in flow rate. The maximum changes in C_d are 6.26 % and 22.79 % when Q = 1 and 6 m^3/h. This indicates that the fluctuation frequency of the flow state becomes larger with the increase of inlet velocity.

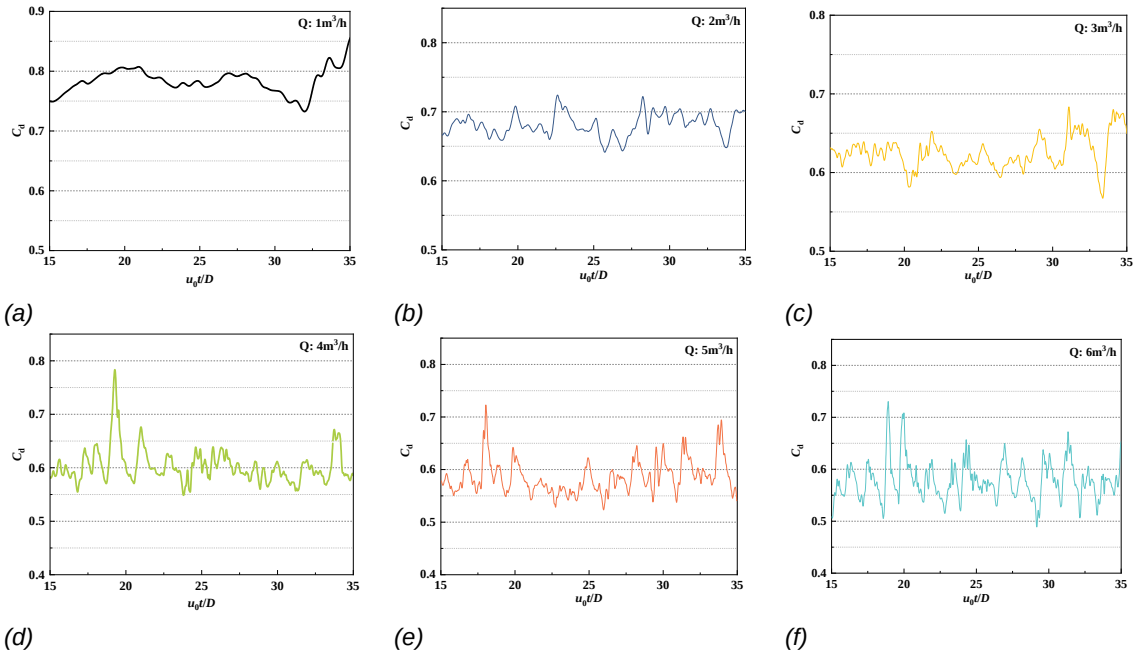

Figure 3: Flow resistance coefficient varies with dimensionless time step (a): Q = 1 m^3/h, (b): Q = 2 m^3/h, (c): Q = 3 m^3/h, (d): Q = 4 m^3/h, (e): Q = 5 m^3/h, (f): Q = 6 m^3/h

The C_L of flow around sphere at Q = 1, 2, 3, 4, 5, and 6 m^3/h are shown in Figure 4. The positive and negative lift coefficients represent the direction of lift force, and the upward direction of lift force is defined as positive. The velocity distributions vertical the flow direction in the X-plane when Q = 2 and 5 m^3/h are shown in Figure 5. It can be seen that the back of the sphere alternately produces up and down shedding vortices. Vortex shedding causes local pressure changes, resulting in pressure differences along the direction perpendicular to the flow direction. Finally, the C_L changes periodically. However, it can be seen that the maximum and minimum values of C_L are constantly changing in an interval. The size and strength of each vortex are different when it falls off, as can be seen in Figure 5. The pressure changes caused by each vortex fall-off are inconsistent. There is a significant phenomenon that the change frequency of the lift coefficient has an obvious difference when the flow rate is different. It can be seen that the increase of inlet flow significantly improves the vortex shedding frequency by combining with Figure 5. The vortex shedding frequency is 0.769 - 1 Hz when the Q = 2 m^3/h and the frequency is 2.04 - 2.60 Hz when Q = 5 m^3/h. The frequency of vortex shedding is about 2.6 times faster.
The heat transfer characteristics of flow around the sphere will be analysed in the following part. The *Nusselt number on the sphere surface varies with flow time when Q = 1, 2, 3, 4, 5, and 6 m^3/h* are shown in Figure 6. It can be seen that the *Nu* is not a stable value, but varies with the flow time. Consistent with the flow characteristics, the fluctuation frequency of *Nu* increased with the increase of inlet flow rate. In addition, the increase in inlet flow improves the *Nu* on the sphere surface. The time-averaged values of *Nu* are: 42.98, 60.82, 74.24, 86.93, 96.85, and 110.48 when *Q = 1, 2, 3, 4, 5, and 6* m^3/h, respectively. That indicates that the increase of inlet velocity will improve the heat transfer performance and increase the volatility of the heat transfer performance of flow around the sphere.

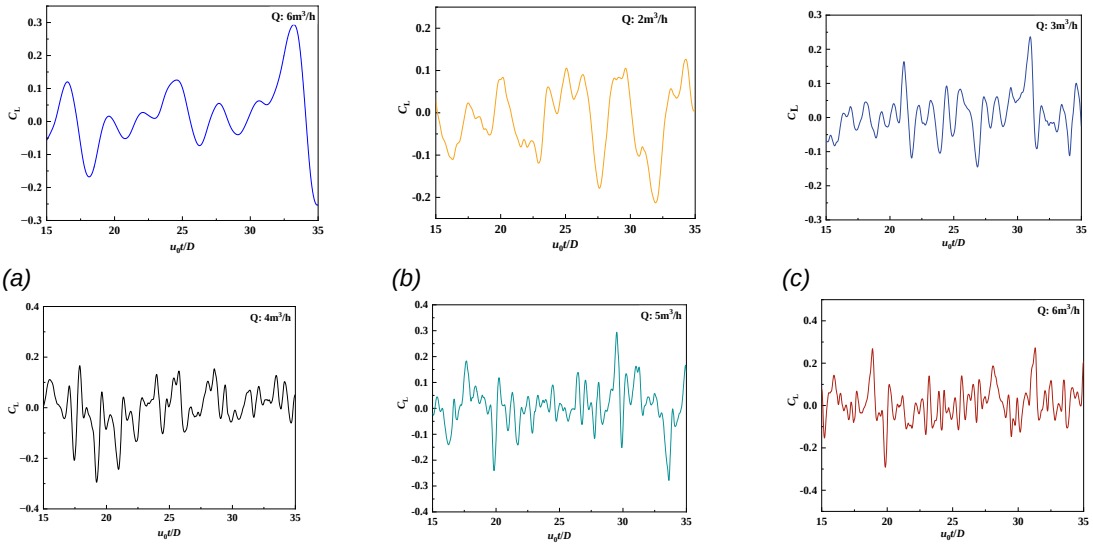

Figure 4: Lift coefficient varies with dimensionless time step (a): Q = 1 m³/h, (b): Q = 2 m³/h, (c): Q = 3 m³/h, (d): Q = 4 m³/h, (e): Q = 5 m³/h, (f): Q = 6 m³/h

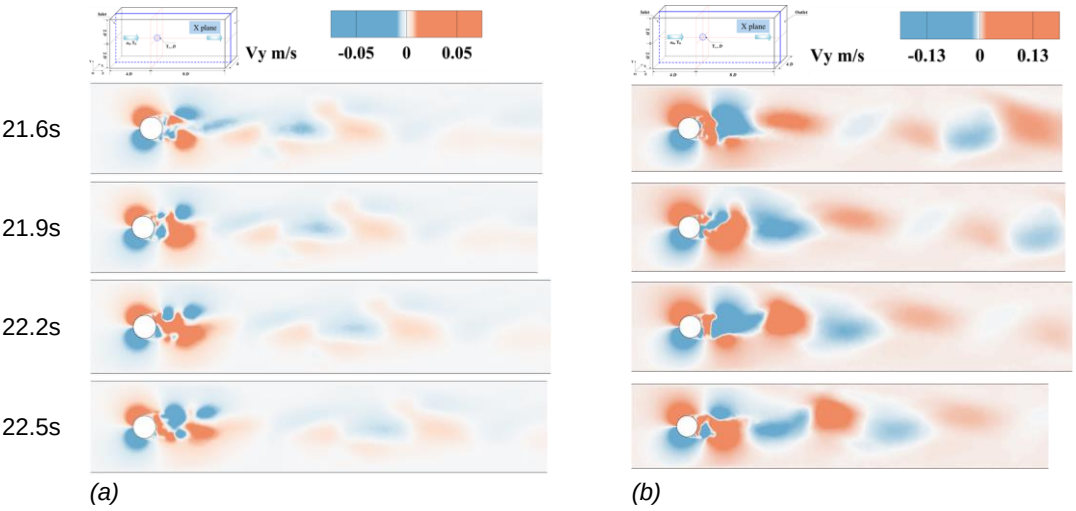

Figure 5: Velocity distributions vertical the flow direction in the X-plane (a) Q = 2 m³/h, (b) Q = 5 m³/h

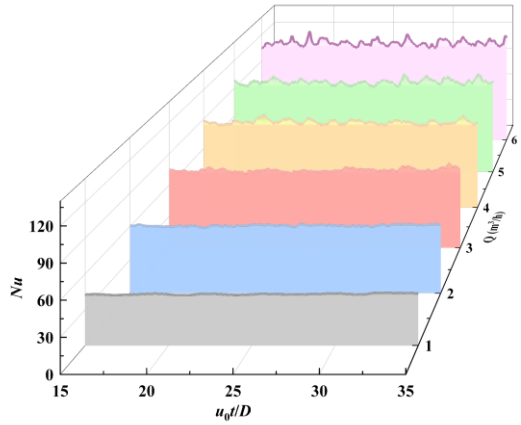

Figure 6: The Nusselt number on the sphere surface varies with dimensionless time step

5. Conclusions

In the present study, the flow and heat transfer characteristics of flow around the sphere are investigated by large eddy simulation. The flow resistance coefficient, lift coefficient and Nusselt number are compared and analysed in detail. The major findings are summarized as follows:

(i) Within the flow rate range studied, the flow around the sphere is a transient process. The C_d, C_L, and Nu fluctuate around a stable value. In addition, the frequency and amplitude of the fluctuation increase significantly as the inlet flow increases. Especially, the maximum changes in C_d are 6.26 % and 22.79 % when Q = 1 and 6 m^3/h. The frequency of vortex shedding increases by about 2.6 times when the flow rate increases from 2 m^3/h to 5 m^3/h.

(ii) Along the flow direction, the leeward region of the sphere alternately produces up and down shedding vortices. Vortex shedding causes local pressure changes, resulting in pressure differences along the direction perpendicular to the flow direction. The transient development of the flow characteristics is caused by the change in the local strength of the shedding vortex.

(iii) The increase in inlet flow rate improves the heat transfer performance of the sphere surface. The increase in flow rate leads to an increase in vortex shedding frequency. The vortex shedding from the leeward region moves downstream with more energy and eventually leads to more cold fluid participating in heat transfer.

The current research shows that the shedding and development of the vortex is a transient process. The strength and energy of the shedding vortices in the leeward region are different and have a great influence on the flow and heat transfer performance. Therefore, it is necessary to study vortex shedding and its development through visualisation experiments. In addition, the flow around the dimpled sphere is deserved to study to find the mechanism of the dimpled structure enhancing heat transfer performance. This is the next step of this research.

Acknowledgements

The work is financially supported by the National Natural Science Foundation of China (No. 52076169).

References

Cocetta F., Gillard M., Szmelter J., Smolarkiewicz P.K., 2021, Stratified flow past a sphere at moderate Reynolds numbers. Computers and Fluids, 226, 104998.

Dixon A.G., Taskin M.E., Nijemeisland M., Stitt E.H., 2011, Systematic mesh development for 3D CFD simulation of fixed beds: Single sphere study. Computers and Chemical Engineering, 35, 1171-1185.

Jia H.N., Zhu F., Tian X., Guo Z.G., Yang J., Wang Q.W., 2022, Numerical investigation of heat transfer enhancement with dimpled particles in structured packed beds. Heat Transfer Research, 53, 19-40.

Li S.Y., Yang J., Wang Q.W., 2017, Large eddy simulation of flow and heat transfer past two side-by-side spheres. Applied Thermal Engineering, 121, 810-819.

Li S.Y., Zhou L., Yang J., Wang Q.W., 2018, Numerical simulation of flow and heat transfer in structured packed beds with smooth or dimpled spheres at low channel to particle diameter ratio. Energies, 111-115.

Nessi E., Dimolian M., Papadopoulos A.I., Ntourou G., Voutetakis S., Intzes K., Dimitriadis, G., Seferlis P., 2022, Experimental testing for calcium carbonate nanoparticles production in a rotating packed bed. Chemical Engineering Transactions, 94, 727-732.

Ranz W.E., Marshall W.R., 1952, Evaporation from drops - Part 1. Chemical Engineering Progress, 48, 141-146.

Sakamoto H., Haniu H., 1990, A study on vortex shedding from spheres in a uniform flow. Transactions of the ASME, 112, 386-392.

Tian X., Jia H.N., Zhang J.Y., Guo Z.G., Yang J., Wang Q.W., 2022, Numerical study on shell-and-tube moving packed bed heat exchanger: Effect of tube arrangement on the particle side. Chemical Engineering Transactions, 60, 187-192.

Whitaker S., 1972, Forced convection heat transfer correlations for flow in pipes, past flat plates, single cylinders, single spheres, and for flow in packed beds and tube bundles. AIChE Journal, 18, 361-371.

Wu Z.H., Wang J.Y., Yang J., Wang Q.W., 2020, Numerical simulation on methane steam reforming in grille-sphere composite packed bed with axial variable diameter configuration particle. Chemical Engineering Transactions, 81, 1177-1182.

Yang J., Zhou L., Hu Y.X., Li, S.Y. Wang Q.W., 2018, Numerical study of forced convective heat transfer in structured packed beds of dimple-particles. Heat Transfer Engineering, 39, 1585-1595.